Molecular Crystals and Liquid Crystals

ISSN: 1542-1406 (Print) 1563-5287 (Online) Journal homepage: http://www.tandfonline.com/loi/gmcl20

Synthesis, Characterization, and Luminescent Property of Amide Functionalized Ruthenium(II) Complexes

Cigdem Sahin

To cite this article: Cigdem Sahin (2015) Synthesis, Characterization, and Luminescent Property of Amide Functionalized Ruthenium(II) Complexes, Molecular Crystals and Liquid Crystals, 607:1, 250-263, DOI: 10.1080/15421406.2014.939573

To link to this article: http://dx.doi.org/10.1080/15421406.2014.939573

Published online: 26 Feb 2015.

Mol. Cryst. Liq. Cryst., Vol. 607: pp. 250–263, 2015

ISSN: 1542-1406 print/1563-5287 online
DOI: 10.1080/15421406.2014.939573

Taylor & Francis
Taylor & Francis Group

Synthesis, Characterization, and Luminescent Property of Amide Functionalized Ruthenium(II) Complexes

CIGDEM SAHIN*

Department of Chemistry, Art & Science Faculty, Pamukkale University, Denizli, Turkey

Amide functionalized bipyridine ligands and their ruthenium(II) complexes of the type [Ru(bipyridine)$_2$(L)](PF$_6$)$_2$ were synthesized and characterized by UV/Visible, emission, FTIR, ^{1}H NMR spectroscopies and elemental analysis. Thermal properties of the ruthenium(II) polypyridyl complexes have been investigated using thermogravimetric analysis (TGA) and differential thermal analysis (DTA) techniques. These complexes show remarkable thermal stability at high temperatures under nitrogen atmosphere. The ruthenium(II) complexes show increasing fluorescence intensity in the presence of the amide groups. The increase of the emission intensity and quantum yield of the molecules may be attributed to the change of dipole moment of the amide group on electronic excitation. The effects of substituent (−CH$_3$, −OCH$_3$, −COOC$_2$H$_5$, −COOH) on photophysical properties of molecules were correlated with the Hammett Substituent Constants. The molecules exhibit linear correlation for absorption and emission maxima.

Keywords Amide group; bipyridine; hydrogen bonding; ruthenium(II) complexes

Introduction

The 2,2′-bipyridine-based ligands have played an important role in coordination chemistry due to forming complexes with many transition metals [1]. Among the transition metal complexes, ruthenium polypyridyl complexes are attracting interest because of their applications [2] in nc- TiO_2 based dye sensitized solar cells (nc-DSSCs) [3], organic light-emitting diodes (OLEDs) [4], biosensors [5], molecular wires [6], and DNA structure probes [7]. Ruthenium(II) polypyridyl complexes containing 4,4′-dicarboxy-2,2′-bipyridine as a photosensitizer attached to nanocrystalline TiO_2 have been widely studied in solar energy conversion processes due to their stability, photophysical, photochemical, and electrochemical properties [8, 9]. The ruthenium(II) polypyridyl complexes are good candidates for OLEDs because of their phosphorescence emission that results in the red-orange region [10]. This application of ruthenium complexes is related to the strong orange-red triplet metal ligand charge transfer (^{3}MLCT) emission, high luminescence quantum yield

*Address correspondence to Cigdem Sahin, Department of Chemistry, Art & Science Faculty, Pamukkale University, Denizli, Turkey. Tel.: +90 258 2963526; Fax: +90 258 2963535. E-mail: cigdemsahin82@gmail.com

Color versions of one or more of the figures in the article can be found online at www.tandfonline.com/gmcl.

and the reversible redox processes [11]. The efficiency of an organic light emitting diode strongly depends on the choice of molecules which can improve performance and stability of an OLED [4]. One of the most used ruthenium complexes in OLED applications is tris-bipyridyl ruthenium(II) complex $[Ru(bpy)_3]^{2+}$ [12]. However, the compounds containing amide groups are rare used as light emitting materials. The lone electron pairs on nitrogen in amide groups can delocalize into the carbonyl group and lead the change of the dipole moment of amide group on electronic excitation. This electronic polarization influences electroluminescence properties of the compounds [12, 13]. Furthermore, the amide groups affect nonradiative decay pathways of the electronic excited state of the ruthenium complexes [14]. Our aim in synthesis of ruthenium(II) complex containing amide groups on bipyridine ligands is to increase the emission intensity and quantum yield of the molecules which are important for OLED application. The present study reports the synthesis and characterization of amide functionalized bipyridine ligands and their ruthenium(II) complexes. The correlation of the photophysical properties with Hammett substituent constants has been investigated. The spectroscopic and thermal properties of synthesized molecules suggest that these molecules can be utilized in OLED applications.

Experimental

Materials

Ruthenium(III) chloride hydrate, 4,4′-dimethyl-2,2′-bipyridine, p-toluidine, 3,5-dimethoxyaniline, and chromiumtrioxide were obtained from Aldrich. 2,2′-bipyridine (bpy) and tetrabutyl ammonium hexafluorophosphate ($TBAPF_6$) were purchased from Fluka. Thionyl chloride and 4-aminobenzoic acid were provided by Merck. $[Ru(bpy)_2Cl_2]\cdot 2H_2O$ and $[Ru(bpy)_3](PF_6)_2$ were prepared according to the literature methods [15, 16]. All reactions and manipulations were carried out under an argon atmosphere using standard Schlenk techniques. Solvents were dried and distilled under a nitrogen atmosphere prior to use. All other chemicals were used as received. The molecular structures of the ruthenium(II) complexes are given in Scheme 1.

Measurements

UV-Vis and fluorescence spectra were recorded in a 1 cm path length quartz cell using an Shimadzu UV-1601 UV-Vis spectrophotometer and Perkin Elmer LS55 fluorescence spectrometers, respectively. The spectra were measured in acetonitrile at a concentration of 4×10^{-5} M. Infrared spectra were recorded on a Perkin Elmer Spectrum Two FT-IR Spectrometer with a diamond ATR. NMR spectra were recorded at probe temperature on a Varian Mercury AS 400 NMR instrument. The reported chemical shifts are referenced to tetramethylsilane (TMS). Elemental analyses were performed using a Carlo Erba 1106 elemental analyzer. The thermal properties of the complexes were obtained by a Shimadzu DTG-60 equipped with DTA and TGA units under nitrogen atmosphere.

Synthesis of Ethyl-4-aminobenzoate

4-aminobenzoic acid (300 mg, 2.19 mmol) and sulfuric acid (0.25 mL) in ethanol (5 mL) was refluxed for 5 h. After cooling of the mixture to room temperature, sodium carbonate solution was added until the solution was neutralized. The resulting product was collected on a sintered glass crucible by suction filtration and was obtained as white solid (60%

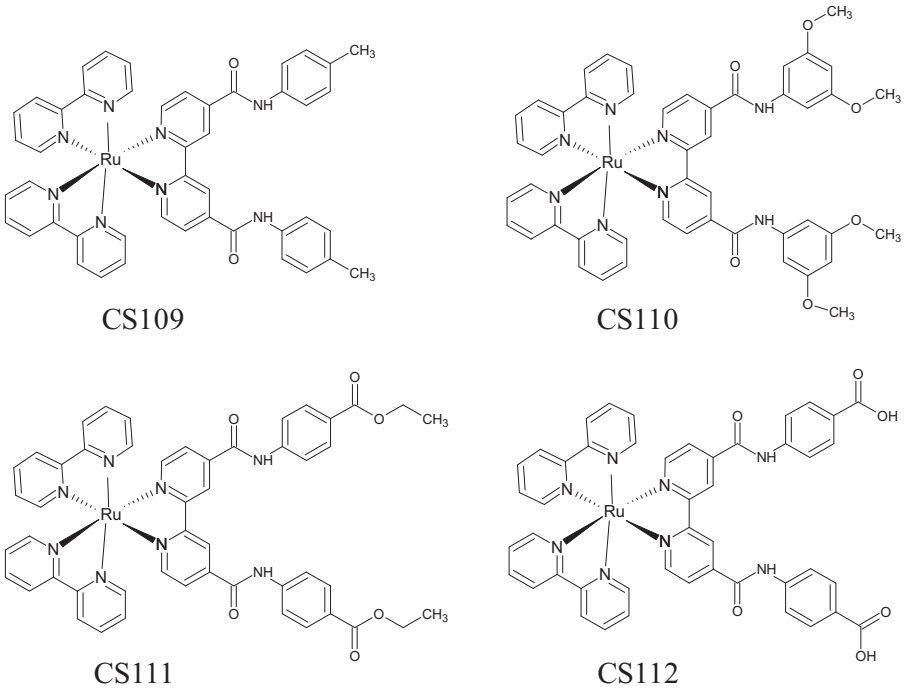

Scheme 1. Molecular structures of the ruthenium(II) complexes.

yield). ^{1}H NMR ($CDCl_3$) δ ppm: 7.80 (d, $J = 8.7$ Hz, 2H), 6.59 (d, $J = 8.7$ Hz, 2H), 4.25 (q, $J = 7.0$ Hz, 2H), 4.01 (s, 2H), 1.31 (t, $J = 6.8$ Hz, 3H). ^{13}C NMR ($CDCl_3$) δ ppm: 166.8, 151.2, 131.6, 120.5, 113.9, 60.3, 14.5.

Synthesis of 4,4′-Dicarboxy-2,2′-bipyridine

Starting from 4,4′-methyl-2,2′-bipyridine was synthesized according to the literature [17]. The product was purified and characterized as 4,4′-dicarboxy-2,2′-bipyridine [9]. The yield was 96%. FTIR (ATR, cm^{-1}): 3449, 1719, 1604, 1563, 1290. ^{1}H NMR (D_2O+NaOH) δ ppm: 7.73 (d, $J = 5.2$ Hz, 2H), 8.24 (s, 2H), 8.64 (d, $J = 5.2$ Hz, 2H). ^{13}C NMR (D_2O+NaOH) δ ppm: 173.2, 155.9, 149.9, 146.6, 123.5, 121.5.

Synthesis of 2,2′-Bipyridine-4,4′-dicarbonyl dichloride

4,4′-dicarboxy-2,2′-bipyridine (400 mg, 1.64 mmol) and thionyl chloride (10 mL) were reflux for 18 h. The excess of thionyl chloride was evaporated under reduced pressure. The product was obtained a pale yellow solid with 98% yield. This product was used without further purification.

Synthesis of 4,4′-Bis[(4-methylphenyl)carbamoyl]-2,2′-bipyridine (1)

4,4′-bis[(4-methylphenyl)carbamoyl]-2,2′-bipyridine was synthesized by modification of literature procedure [18]. P-toluidine (41 mg, 0.38 mmol) was dissolved in dry dichloromethane (10 mL) under argon. Then 2,2′-bipyridine-4,4′-dicarbonyl dichloride

(50 mg, 0.18 mmol) was added in five portions over a period of 1 h. The mixture was stirred at room temperature for 8 h. The resulting product was collected on a sintered glass crucible by suction filtration. The solid was washed with distilled water and diethyl ether. The compound was obtained as a white powder. Yield: 50%. FTIR (ATR, cm^{-1}): 3282, 3113, 3037, 2919, 1647, 1597, 1553, 1526, 1364, 1266, 1011. ^{1}H NMR (DMSO-d_6, 400MHz) δ ppm: 10.59 (s, 2H), 8.93 (d, $J = 4.0$ Hz, 2H), 8.88 (s, 2H), 7.96 (d, $J = 4.0$ Hz, 2H), 7.67 (d, $J = 8.1$ Hz, 4H), 7.18 (d, $J = 8.1$ Hz, 4H), 2.48 (s, 6H). Anal. Calcd. for $C_{26}H_{22}N_4O_2$(%): C, 73.92; H, 5.25; N, 13.26. Found: C, 73.95; H, 5.23; N, 13.28.

Synthesis of 4,4′-Bis[(3,5-dimethoxyphenyl)carbamoyl]-2,2′-bipyridine (2)

4,4′-bis[(3,5-dimethoxyphenyl)carbamoyl]-2,2′-bipyridine was synthesized from 3,5-dimethoxyaniline (58 mg, 0.38 mmol) and 2,2′-bipyridine-4,4′-dicarbonyl dichloride (50 mg, 0.18 mmol) by using the same reaction procedure of compound 1. Yield: 54%. FTIR (ATR, cm^{-1}): 3270, 3114, 2933, 2836, 1659, 1598, 1536, 1365, 1295, 1156, 1012. ^{1}H NMR (DMSO-d_6, 400 MHz) δ ppm: 10.61 (s, 2H), 8.96 (d, $J = 5.2$ Hz, 2H), 8.89 (s, 2H), 7.96 (d, $J = 5.2$ Hz, 2H), 7.11 (d, $J = 2.4$ Hz, 4H), 6.33 (s, 2H), 3.76 (s, 12H). Anal. Calcd. for $C_{28}H_{26}N_4O_6$(%): C, 65.36; H, 5.09; N, 10.86. Found: C, 65.40; H, 5.14; N, 10.89.

Synthesis of 4,4′-Bis[(4-(ethoxycarbonyl)phenyl)carbamoyl]-2,2′-bipyridine (3)

4,4′-bis[(3,5-dimethoxyphenyl)carbamoyl]-2,2′-bipyridine was synthesized from ethyl-4-aminobenzoate (63 mg, 0.38 mmol) and 2,2′-bipyridine-4,4′-dicarbonyl dichloride (50 mg, 0.18 mmol) by using the same reaction procedure of compound 1. Yield: 52%. FTIR (ATR, cm^{-1}): 3312, 3113, 2986, 2907, 1711, 1655, 1601, 1552, 1523, 1365, 1279, 1170, 1011. ^{1}H NMR (DMSO-d_6, 400MHz) δ ppm: 10.99 (s, 2H), 8.98 (d, $J = 4.4$ Hz, 2H), 8.92 (s, 2H), 7.99 (d, $J = 4.8$ Hz, 4H), 7.91 (d, $J = 4.8$ Hz, 6H), 4.31 (q, $J = 4.4$ Hz, 4H), 1.34 (t, $J = 7.6$, 7.2 Hz, 6H). Anal. Calcd. for $C_{30}H_{26}N_4O_6$(%): C, 66.51; H, 4.87; N, 10.40. Found: C, 66.56; H, 4.83; N, 10.45.

Synthesis of 4,4′-Bis[(4-(hydroxycarbonyl)phenyl)carbamoyl]-2,2′-bipyridine (4)

4,4′-bis[(3,5-dimethoxyphenyl)carbamoyl]-2,2′-bipyridine was synthesized from 4-aminobenzoic acid (39 mg, 0.29 mmol) and 2,2′-bipyridine-4,4′-dicarbonyl dichloride (40 mg, 0.14 mmol) by using the same reaction procedure of compound 1. Yield: 56%. FTIR (ATR, cm^{-1}): 3313, 3114, 2920, 2780, 1711, 1658, 1603, 1562, 1364, 1282, 1170, 1011. ^{1}H NMR (DMSO-d_6, 400MHz) δ ppm: 10.95 (s, 2H), 8.95 (d, $J = 4.4$ Hz, 2H), 8.91 (s, 2H), 7.95 (d, $J = 4.8$ Hz, 4H), 7.90 (d, $J = 4.8$ Hz, 6H). Anal. Calcd. for $C_{30}H_{26}N_4O_6$(%): C, 64.73; H, 3.76; N, 11.61. Found: C, 64.77; H, 3.73; N, 11.64.

Synthesis of [Ru(bpy)$_2$(1)](PF$_6$)$_2$ (CS109)

[Ru(bpy)$_2$Cl$_2$].2H$_2$O (13.5 mg, 0.028 mmol) and compound 1 (11.4 mg, 0.028 mmol) were heated under reflux in ethanol (15 mL) for 10 h under argon. The solution was concentrated to 5 mL and then aqueous solution of KPF_6 was added into the mixture. The brown precipitate was collected by filtration. The product was washed with water followed by ether and then dried in air. Yield: 62%. FTIR (ATR, cm^{-1}): 3390, 3121, 3085, 2979, 2937, 2878, 1644, 1604, 1567, 1542, 1446, 1314, 1243, 1023, 832, 761, 556. ^{1}H NMR (Acetone-d_6, 400 MHz) δ ppm: 9.46 (s, 2H), 8.86 (d, $J = 7.6$ Hz, 6H), 8.30 (d, $J = 5.6$ Hz,

2H), 8.26 (m, 4H), 8.13 (d, $J = 6.0$ Hz, 2H), 8.09 (d, $J = 4.8$ Hz, 2H), 8.04 (d, $J = 4$ Hz, 2H), 7.68 (d, $J = 8.8$ Hz, 4H), 7.61 (m, 4H), 7.21 (d, $J = 8$ Hz, 4H), 2.32 (s, 6H). Anal. Calcd. for $C_{46}H_{38}N_8O_2RuP_2F_{12}$(%): C, 49,07; H, 3.40; N, 9.95. Found: C, 49,02; H, 3.36; N, 9.90.

CS110, CS111, and CS112 were synthesized starting from compounds 2, 3, and 4, respectively, by using the same reaction conditions and purification steps of CS109.

Synthesis of [Ru(bpy)$_2$(2)](PF$_6$)$_2$ (CS110)

The compound was obtained as a brown powder. Yield: 67%. FTIR (ATR, cm^{-1}): 3393, 3113, 3101, 2939, 2937, 2843, 1682, 1603, 1548, 1460, 1365, 1283, 1154, 1067, 834, 764, 556. ^{1}H NMR (Acetone-d$_6$, 400 MHz) δ ppm: 9.58 (s, 2H), 8.85 (d, $J = 7.6$ Hz, 4H), 8.29 (d, $J = 6.0$ Hz, 4H), 8.25 (m, 4H), 8.12 (d, $J = 5.6$ Hz, 2H), 8.08 (d, $J = 5.6$ Hz, 2H), 8.02 (dd, $J = 1.6$ Hz, 2H), 7.59 (m, 4H), 7.14 (s, 4H), 7.14 (s, 2H), 6.33 (s, 2H), 3.77 (s, 12H). Anal. Calcd. for $C_{48}H_{42}N_8O_6RuP_2F_{12}$ (%): C, 47,34; H, 3.48; N, 9.20. Found: C, 47.28; H, 3.49; N, 9.23.

Synthesis of [Ru(bpy)$_2$(3)](PF$_6$)$_2$ (CS111)

The compound was obtained as a brown powder. Yield: 63%. FTIR (ATR, cm^{-1}): 3383, 3114, 3102, 2984, 2937, 2907, 1717, 1682, 1600, 1529, 1365, 1278, 1104, 1013, 834, 764, 556. ^{1}H NMR (Acetone-d$_6$, 400 MHz) δ ppm: 9.56 (s, 2H), 8.86 (d, $J = 8.4$ Hz, 4H), 8.33 (d, $J = 6$ Hz, 2H), 8.25 (m, 4H), 8.12 (d, $J = 6$ Hz, 2H), 8.08 (t, $J = 6.8$, 6 Hz, 4H), 8.03 (d, $J = 8.4$ Hz, 5H), 7.97 (d, $J = 9.2$ Hz, 5H), 7.61 (m, 4H), 4.34 (q, $J = 6.8$ Hz, 4H), 1.36 (t, $J = 6.8$, 7.2 Hz, 6H). Anal. Calcd. for $C_{50}H_{42}N_8O_6RuP_2F_{12}$ (%): C, 48,36; H, 3.41; N, 9.02. Found: C, 48.33; H, 3.37; N, 9.06.

Synthesis of [Ru(bpy)$_2$(2)](PF$_6$)$_2$ (CS112)

The compound was obtained as a brown powder. Yield: 69%. FTIR (ATR, cm^{-1}): 3383, 3117, 386, 2970, 2931, 2872, 1728, 1644, 1605, 1545, 1467, 1370, 1264, 1167, 1108, 1024, 808, 553. ^{1}H NMR (Acetone-d$_6$, 400 MHz) δ ppm: 9.53 (s, 2H), 8.84 (d, $J = 8.4$ Hz, 4H), 8.31 (d, $J = 6$ Hz, 2H), 8.25 (m, 4H), 8.13-7.94 (m, 16H), 7.59 (m, 4H). Anal. Calcd. for $C_{46}H_{34}N_8O_6RuP_2F_{12}$ (%): C, 46.59; H, 2.89; N, 9.45. Found: C, 46.61; H, 2.90; N, 9.40.

Results and Discussion

Synthesis and Structural Characterization

The summary of the synthetic route for the synthesized materials is shown in Scheme 2. 4,4′-dimethyl-2,2′-bipyridine was oxidized to 4,4′-dicarboxy-2,2′-bipyridine which was converted into 2,2′-bipyridine-4,4′-dicarbonyl dichloride in the presence of the excess thionyl chloride. Amide functionalized bipyridine ligands were obtained from the condensation between 2,2′-bipyridine-4,4′-dicarbonyl dichloride and 2.1 equiv of the aromatic amines. The reactions were conducted in anhydrous dichloromethane and at low temperature to achieve a clean reaction without undesirable product [19]. The reaction of $[Ru(bpy)_2Cl_2]\cdot 2H_2O$ with amide functionalized bipyridine derivatives followed by the addition of an aqueous solution of KPF_6 to precipitate the products. The complexes were obtained as a brown powder with 62–69% yield.

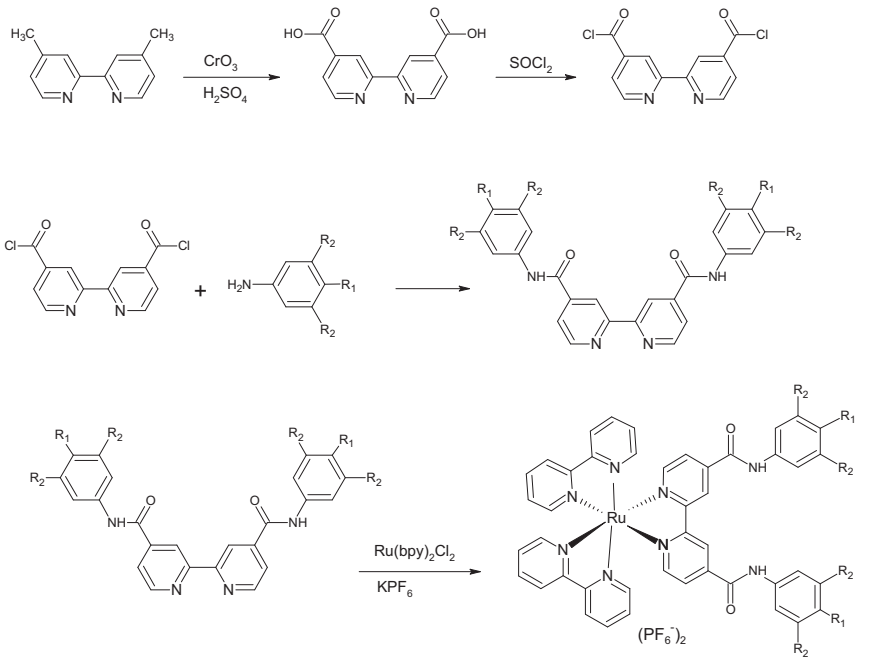

CS109: $R_1 = CH_3$; $R_2 = H$ **CS111:** $R_1 = COOCH_2CH_3$; $R_2 = H$

CS110: $R_1 = H$; $R_2 = OCH_3$ **CS112:** $R_1 = COOH$; $R_2 = H$

Scheme 2. The synthetic route for ligands and ruthenium(II) complexes.

The structures of synthesized ligands and complexes were confirmed by FT-IR, ^{1}H NMR spectroscopies. The FT-IR spectra of ligands (1–4) indicate characteristics the N–H stretching bands and carbonyl group of amide bands between 3312–3282 and 1647–1659 cm^{-1}, respectively [20]. The peaks at 1711 cm^{-1} are assigned to the carbonyl ν(C=O) group bands for ligands 3 and 4. The remaining peaks in the range 1010–1600 cm^{-1} are attributable to ν(C−O) and ring stretching of the ligands. In the FT-IR spectra of the ruthenium complexes (CS109, CS110, CS111, CS112), the bands for the stretching vibrations of amide group (C=O) and (N−H) are shifted to higher wavenumbers by about 25 cm^{-1} compared to free ligands. The absorption band at 556 cm^{-1} relative to Ru-N bond is observed, when the bipyridine ligands coordinate to ruthenium metal [21].

The ^{1}H NMR spectrum of ligand 1 (Fig. 1) shows signals attributable to the amide N−H and methyl proton signals as singlets at 10.60 ppm and 2.48 ppm, respectively. Characteristic proton signals of methoxy substituents of ligand 2 are observed as singlets at 3.76 ppm. In ligands 3 and 4 containing electron-withdrawing ethoxycarbonyl and hydroxycarbonyl groups on phenyl ring lead to a downshift of amide protons. The ^{1}H NMR spectrum of complex CS109 (Fig. 1) shows 8 resonance peaks relative to bipyridine rings in the aromatic region, although it was expected to give 11 proton signals. It is attributed to different magnetic environments of the pyridine rings on the bipyridine ligands. The proton signals of the pyridine rings can overlap and appear nearly equivalent [22]. In the complex CS109, the amide proton signal in the aromatic region, and the methyl resonance peaks in the aliphatic region are shifted upfield compared to free ligand. In the ^{1}H NMR spectra of

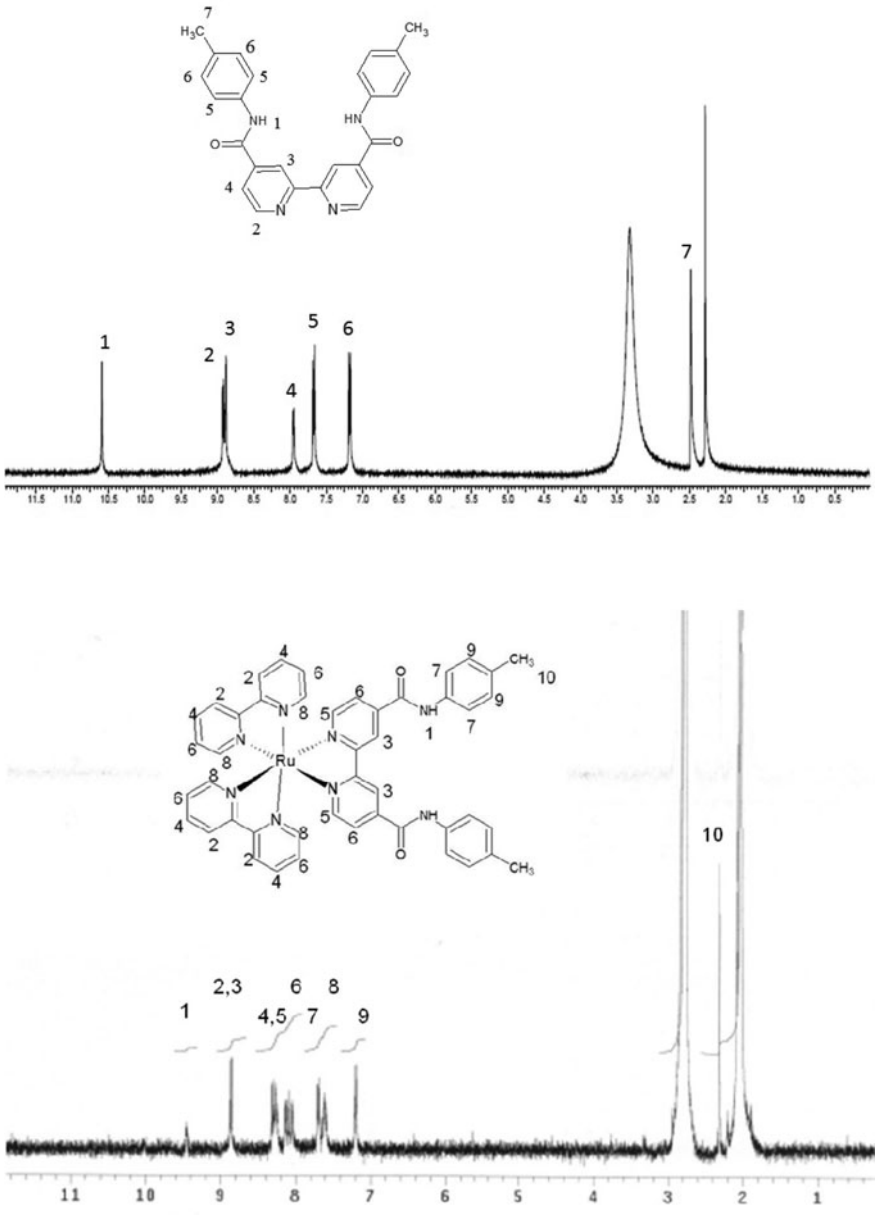

Figure 1. ^{1}H NMR spectra of ligand 1 in DMSO-d_6 and CS109 complex in acetone-d_6.

other complexes (CS110, CS111, CS112), the ratios of aromatic resonance peaks prove the presence of three bipyridine ligands and two phenyl rings.

Absorption and Emission Studies

The UV-Vis absorption of ruthenium complexes in acetonitrile solvent are shown in Fig. 2. The maximum absorption wavelengths and the molar extinction coefficients are summarized

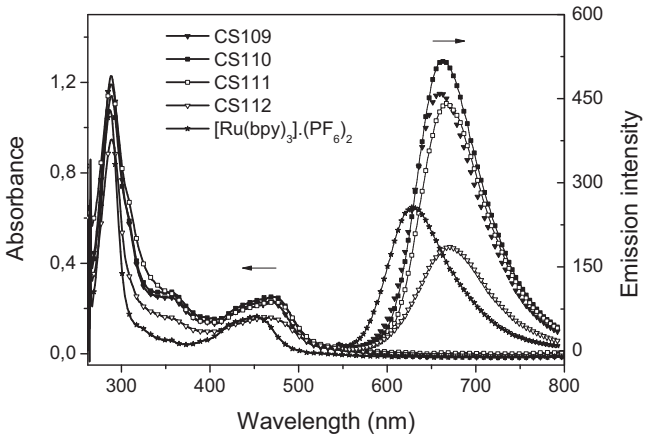

Figure 2. UV-Vis absorption and emission spectra of 4×10^{-5} M solution of the ruthenium(II) complexes in acetonitrile.

in Table 1. The absorption spectra of the ruthenium complexes show the bands in the range 288–480 nm. The absorption bands at 288 nm correspond to the π-π^* ligand-centered charge transfer (LC) transitions of bipyridine ligands and the visible bands around 480 nm are assigned to metal to ligand charge transfer (MLCT) transitions [23]. The lowest energy MLCT absorption bands are attributed to the transition from a filled dπ metal orbital (t_{2g}) to a empty ligand-based orbital (π^*) [24]. The complexes show an additional band at 360 nm due to the presence of the amide groups [25]. These spectra are similar to $[Ru(bpy)_3](PF_6)_2$ complex, except red shift in the MLCT bands. The red shift is attributed to the electron withdrawing characteristics of the amide groups lowering the energy MLCT transitions [18].

Table 1. Absorption and emission data of the Ru(II) complexes

		λ_{mx}^{abs}, (nm) ($\varepsilon/10^4$)			λ_{mx}^{em}(nm)			Φ_{em}
Complex	σ_p	($M^{-1}.cm^{-1}$) (CH_3CN)			(CH_2Cl_2)	(CH_3CN)	(CH_3OH)	(CH_3CN)
CS109		288	359	472	650	658	673	0.15
	−0.07	(3.06)	(0.61)	(0.58)				
CS110	0.12	289	359	475	654	661	672	0.15
		(2.85)	(0.68)	(0.63)				
CS111	0.45	289	360	480	660	665	676	0.14
		(2.99)	(0.67)	(0.59)				
CS112	0.45	289	360	479	663	667	686	0.092
		(2.38)	(0.40)	(0.40)				
$[Ru(bpy)_3]$ $(PF_6)_2$		287	451		608	624	618	0.095
		(2.69)	(0.42)					

The emission spectra of the Ru(II) complexes were obtained in different solvents by excitation at 480 nm. σ_p values obtained from [31].

The emission spectra of the ruthenium complexes (Fig. 2) were obtained at room temperature in acetonitrile. The ruthenium complexes exhibit broad emission band due to the ^{3}MLCT state [14]. The emission maximum of ruthenium(II) polypridyl complexes containing amide groups were red-shifted by 33 nm compared to $[Ru(bpy)_3](PF_6)_2$ complex. The stronger acceptor property of the amide group on bipyridine ligand decreases the energy of the excited state [18]. The emission quantum yield of ruthenium complexes were calculated according to Eq. (1), where Φ_f is the fluorescence quantum yield, A is the absorption intensity, S is the integrated emission band area, and n is the solvent reflective index, u and s refer the unknown and standard, respectively [26]

$$\phi_{\mathrm{f}} = \phi_{\mathrm{fs}} \frac{S_u}{S_s} \frac{A_s}{A_u} \frac{n_u^2}{n_s^2}. \tag{1}$$

The fluorescence quantum yield measurements for solutions were prepared in acetonitrile and $[Ru(bpy)_3](PF_6)_2$ was used as the reference materials ($\Phi_f = 0.095$ in acetonitrile) [27]. In comparison with $[Ru(bpy)_3](PF_6)_2$ complex, there is an important difference in the emission intensities and quantum yields of the complexes (CS109, CS110, CS111). The emission intensities of these complexes are 1.7–2.5 times higher than the $[Ru(bpy)_3](PF_6)_2$ complex and they exhibit high fluorescence quantum yield ($\Phi_f = 0.15$–0.14), except for CS112 complex. The increase of the emission intensity and quantum yield of the molecules may be attributed to the change of dipole moment of the amide group on electronic excitation [12, 13]. This electronic polarization allows the π extended electron system between amide bond and aromatic rings [12, 13]. Although it was expected that complex CS112 may have similar emission properties like other complexes (CS109, CS110, CS111), there is a decrease in the emission intensity and quantum yield of CS112 ($\Phi_f = 0.092$). When the carboxylic acid group binds to an aromatic ring, the carboxylic acid group can be close to the planarity of the ring, and this results in an increase of intramolecular interaction [28]. Therefore, it leads to a decrease in fluorescence.

The emission spectra of the ruthenium complexes in the different polarities of solvents were obtained at room temperature by excitation at 480 nm (Fig. 3). All of the complexes show similar solvatochromic behavior in polar aprotic solvents (dichloromethane and acetonitrile). The emission maxima of the ruthenium complexes are slightly blue-shifted from acetonitrile to dichloromethane with the decreasing polarity of solvents. This shift can be attributed to the less interactions between the excited molecules and solvents [29]. In polar protic solvent (methanol), the compounds containing the aromatic amide groups induce intermolecular hydrogen bonding and lead to spectral red shift. The intermolecular hydrogen bonding also decreases fluorescence intensity due to quenching effect in polar protic solvent [13].

The photoluminescent properties of the complexes may be appropriate to be used as red emitters in OLEDs [4].

Correlation of the Photophysical Properties with Hammett Substituent Constants

Hammett correlations can be used as a useful model to investigate substituents' effect on photophysical properties of molecules [30]. The absorption and emission maxima of the complexes as a function of Hammett Substituent Constants (σ_p) [31] were plotted in Fig. 4. The linear correlations was observed for absorption and emission maxima with regression coefficients $R^2 = 0.9867$ and $R^2 = 0.9589$, respectively. This correlation gives

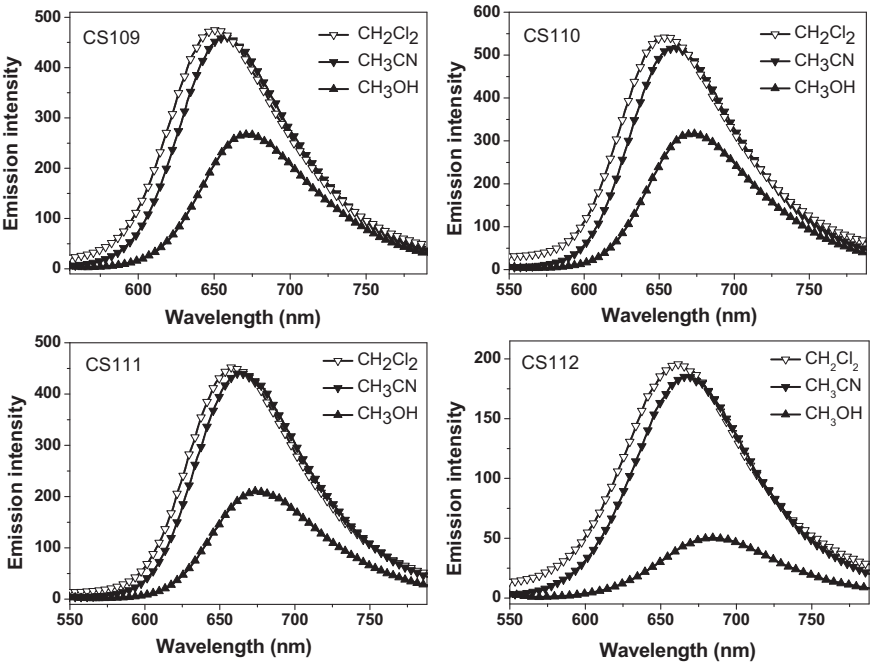

Figure 3. The emission spectra of the ruthenium(II) complexes in different solvents: Acetonitrile (CH_3CN), dichloromethane (CH_2Cl_2), methanol (CH_3OH).

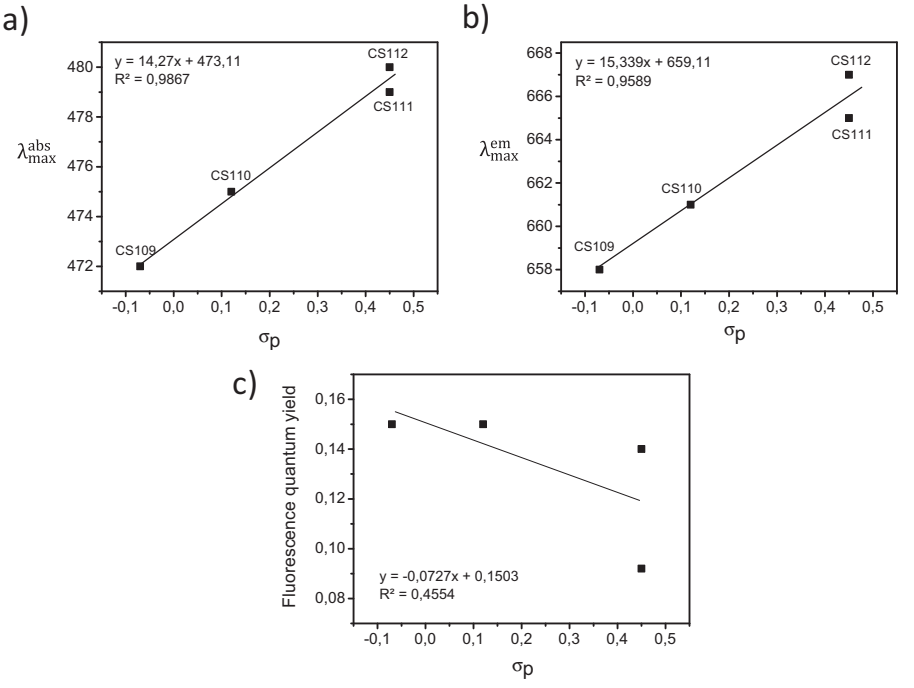

Figure 4. The correlation between σ_p and (a) absorption maxima, (b) emission maxima, (c) fluorescence quantum yield of ruthenium(II) complexes in acetonitrile.

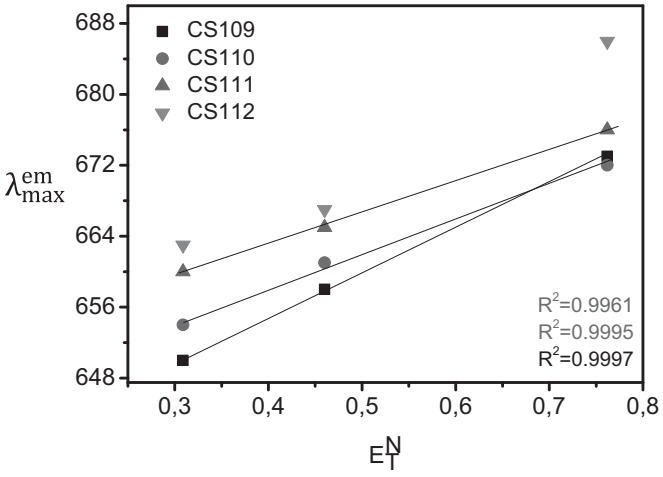

Figure 5. The emission maxima of ruthenium(II) complexes as a function of the normalized molar electronic transition energy (E_T^N). E_T^N (CH_2Cl_2): 0.309, E_T^N (CH_3CN): 0.460, E_T^N (CH_3OH): 0.762 [34].

an opportunity to predict the spectroscopic data of many substituted molecules which σ_p values are known from literature [31, 32]. The electron withdrawing groups (−$COOC_2H_5$, −COOH) linked to aromatic ring in ruthenium complexes (CS111, CS112) make more positive σ_p values of substituents and cause red shift compared to the complexes containing electron donor substituents (CS109, CS110) [33]. The red shift is related to decreasing the band gap between the ground and excited states of molecules. When the substituent effects of molecules (−CH_3, −OCH_3, −$COOC_2H_5$, −COOH) on fluorescence quantum yields were investigated, it was found that there is no correlation between σ_p and fluorescence quantum yield (Fig. 4c).

The emission maxima of the complexes were seen to correlate with the normalized molar electronic transition energy (E_T^N) (Fig. 5) [34]. The regressions were linear for the molecules (CS109, CS110, CS111) in polar aprotic solvents (dichloromethane and acetonitrile) which the emission maxima are red-shifted with increasing the solvent polarity. However, the molecule CS112 shows deviation in polar protic solvent (methanol) due to the interaction of carboxylic acid groups [28].

The Thermal Behavior of the Ruthenium Complexes

The TGA and DTA curves of the ruthenium complex were obtained at heating rate of 20°C/min in the temperature range of 30–900°C under N_2 atmosphere (Fig. 6). The thermoanalytical data of the ruthenium complex are summarized in Table 2. The TGA curve of CS109 shows four decomposition steps in the range 149–782°C (Fig. 6). The first decomposition occurs between 149°C and 160°C with 16.57% mass loss which is attributed to the elimination of 2 mol methyl phenyl units. In the second step, the mass loss of 21.41% was observed between 160°C and 380°C due to the elimination of the one bipyridine ligand containing two amide groups. The mass loss corresponding to the elimination of $2PF_6$ group was 25.11% between 380°C and 595°C in the third step. Finally, mass loss (27.37%) in the temperature range 595–782°C shows the removal of the two bipyridine groups of the complex ($C_{10}H_8N_2$). After this decomposition step, the black colored residue with the mass 9.54% may be assigned to the ruthenium. The DTA curves of CS109 are given in

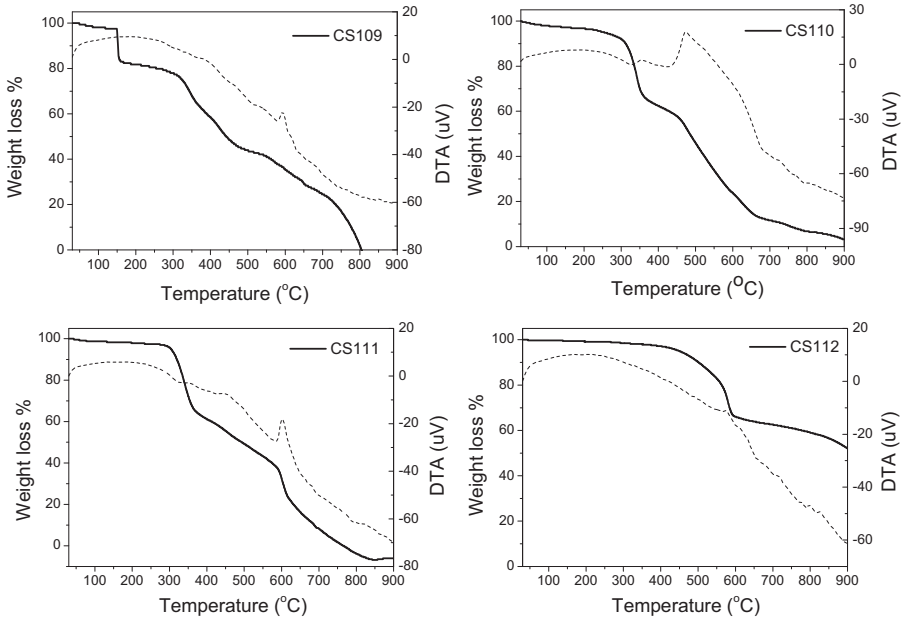

Figure 6. TGA and DTA curves of the ruthenium(II) complexes.

Table 2. Mass loss (%) of the ruthenium(II) complexes in the different temperature ranges

Complex	Stage	TGA temp. range (°C)	Mass loss (%)		Decomposition product loss
			Found	**Calc.**	
CS109	I	149–160	16.57	16.37	$2C_6H_5$-CH_3
	II	160–380	21.41	21.34	$C_{10}H_8N_2$+2CONH
	III	380–595	25.11	25.75	$2PF_6$
	IV	595–782	27.37	27.75	2 $C_{10}H_8N_2$
	Residue	>782	8.98	9.54	Ru
CS110	I	313–350	29.72	29.59	$2C_6H_5$+2CONH +4OCH_3
	II	350–467	12.52	12.82	$C_{10}H_8N_2$
	III	467–868	49.64	49.45	2 $C_{10}H_8N_2$+$2PF_6$
	Residue	>868	8.12	8.29	Ru
CS111	I	305–362	31.85	30.97	$2C_6H_5$+2CONH +2$COOCH_2CH_3$
	II	362–461	12.60	12.58	$C_{10}H_8N_2$
	III	461–800	48.31	48.49	2 $C_{10}H_8N_2$+$2PF_6$
	Residue	>800	7.24	7.96	Ru
CS112	I	390–640	39.82	40.68	$C_{10}H_8N_2$+2CONH +$2C_6H_5$+2COOH
	II	640–900	13.64	13.16	$C_{10}H_8N_2$
	Residue	>900			The mass loss is 53.46% up to 900°C

Fig. 6. The exothermic peaks are observed at 395, 593, and 618°C due the formation of intermediate products [35].

The decomposition temperature range and percentage of mass losses of CS110 and CS111 are listed in Table 2. Thermal behaviors of CS110 and CS111 result in similar decomposition steps which give higher thermal stability than CS109 in the presence of the $–OCH_3$ and $–COOCH_2CH_3$ moieties on phenyl groups. The thermal decomposition of these complexes appears at three steps. The mass loss under 365°C for these complexes are attributed to the $4OCH_3$ ($2COOCH_2CH_3$ for CS111), $2C_6H_5$, and 2CONH groups in the first step. The second decomposition occurs with the elimination of the one bipyridine ligand. In the third step, two bipyridine and $2PF_6$ groups of the complexes undergo decomposition in the temperature range 460–870°C. The complexes exhibit a mass loss above 800°C, corresponding to the formation of Ru as a residue. The exothermic and endothermic peaks are observed from DTA curves of CS110 and CS111 complexes. The peaks are related to the decomposition of ruthenium complexes.

TGA curve of CS112 (Fig. 6) shows interesting thermal behavior in comparison to other complexes (CS109, CS110, CS111). The mass loss of CS112 is 53.46% up to 900°C, although the decomposition of other complexes (CS109, CS110, CS111) occur with around 91% mass loss under 900°C (Table 2). In addition, the CS112 leads to higher thermal degradation temperature (458°C) in the presence of the carboxylic acid group [36]. The enhanced thermal stability is attributed to strong H-bond interaction of carboxylic acid. Furthermore, the exothermic peaks in the DTA curve of CS112 shows that the decomposition of complex shifts to higher temperature due to in the presence of the carboxylic acid group.

Conclusion

The bipyridine ligands containing aromatic amide groups and their ruthenium(II) complexes were synthesized by using simple methods. It was found that the ruthenium(II) complexes show a red shift in emission maximum and an increase in emission intensity in the presence of the amide groups. The effects of substituent on photophysical properties of molecules were investigated by Hammett correlation. The linear correlation was found between spectroscopic data and $\sigma_{p.}$ Thermoanalytical results show that these complexes have high thermal degradation temperature. The new molecules with amide groups can be a good alternative for OLED applications.

Funding

The authors acknowledge the project support fund of Pamukkale University.

References

[1] Rosenthal, J., Nepomnyashchii, A. B., Kozhukh, J., Bard, A. J., & Lippard, S. J. (2011). *J. Phys. Chem. C*, *115*, 17993.
[2] Brito, I., Aguilera, V., Arias, M., Lopez-Rodriguez, M., & Cardenas, A. (2011). *Mol. Cryst. Liq. Cryst.*, *548*, 284.
[3] Chang, D. M., Kwon, D. Y., & Kim, Y. S. (2013). *Mol. Cryst. Liq. Cryst.*, *585*, 91.
[4] Oner, I., Sahin, C., & Varlikli, C. (2012). *Dyes Pigments*, *95*, 23.
[5] Erdem, A., Kerman, K., Meric, B., Ozkan, D., & Kara, P., *et al.* (2002). *Turk. J. Chem*,. *26*, 851.
[6] Barigelletti, F., & Flamigni, L. (2000). *Chem. Soc. Rev.*, *29*, 1.
[7] Shilpa, M., Latha, J. N. L., Devi, A. G., Nagarjuna, A., & Kumar, Y. P., *et al.* (2011). *J. Incl. Phenom. Macrocycl. Chem.*, *70*, 187.

[8] Ocakoglu, K., Yakuphanoglu, F., Durrant, J. R., & Icli. S. (2008). *Sol. Energ. Mat. Sol. Cells*, *92*, 1047.
[9] Sahin, C., Dittrich, T., Varlikli, C., Icli, S., & Lux-Steiner, M. C. (2010). *Sol. Energ. Mater. Sol. Cells*, *94*, 686.
[10] Zhu, Y., Shen, F., Liu, M., Zhang, M., & Ma, Y. (2008). *Semicond. Sci. Technol.*, *23*, 052001.
[11] Zhu, Y., Mab, Y., & Zhu, J. (2013). *J. Lumin.*, *137*, 198.
[12] Li, M., Liu, J., Zhao, C., & Sun, L. (2006). *J. Organomet. Chem.*, *691*, 4189.
[13] Demchenko, A. P., & Yesylevskyy, S. O. (2011). In: *Advanced Fluorescence Reporters in Chemistry and Biology III, Applications in Sensing and Imaging*, Demchenko, A. P. & Wolfbeis, O. S. (Eds.), Chapter 1, Springer: Heidelberg, 3.
[14] Carvalho, I. M. M. D., Sousa Moreira, I. D., & Gehlen, M. H. (2003). *Inorg. Chem.*, *42*, 1525.
[15] Sprintschnik, G., Sprintschnik, H. W., Kirsch P. P., & Whitten, D. G. (1977). *J. Am. Chem. Soc.*, *99*, 4947.
[16] Cooley, L. F., Headford, C. E. L., Elliott, C. M., & Kelley, D. F. (1988). *J. Am. Chem. Soc.*, *110*, 6673.
[17] Garelli, N., & Vierling, P. (1992). *J. Org. Chem.*, *57*, 3046.
[18] Pratt, M. D., & Beer, P. D. (2004). *Tetrahedron*, *60*, 11227.
[19] Liu, Y., Song, Y., Chen, Y., Li, X. Q., Ding, F., *et al.* (2004). *Chem. Eur. J.*, *10*, 3685.
[20] Pearson, P., Bond, A. M., Deacon, G. B., Forsyth, C., & Spiccia, L. (2008). *Inorganica Chimica Acta*, *361*, 601.
[21] Quinby, M. S., & Feltham, R. D. (1972). *Inorg. Chem.*, *11*, 2468.
[22] Yang, X. J., Janiak, C., Heinze J., Drepper, F., Mayer, P., *et al.* (2001). *Inorganica Chimica Acta*, *318*, 103.
[23] Sahin, C., Varlıklı, C., Zafer, C., Shi, Q., & Douthwait, R. E. (2013). *J. Coord. Chem.*, *66*, 1384.
[24] Fantacci, S., Angelis, F. D., & Selloni, A. (2003). *J. Am. Chem. Soc.*, *125*, 4381.
[25] Beer, P. D., Szemes, F., Passaniti, P., & Maestri, M. (2004). *Inorg. Chem.*, *43*, 3965.
[26] Karapire, C., Timur, C., & Sıddık, I. (2003). *Dyes Pigments*, *56*, 135.
[27] Knight, T. E., Goldstein, A. P., Brennaman, M. K., Cardolaccia, T., Pandya, A., *et al.* (2011). *J. Phys. Chem. B*, *115*, 64.
[28] Valeur, B., *et al.* (2012). *Molecular Fluorescence: Principles and Applications*, Wiley-VCH: Weinheim, Germany.
[29] Xu, J., Yang, C., Tong, B., Zhang, Y., Liang, L, *et al.* (2013). *J Fluoresc.*, *23*, 865.
[30] Fernandez, I., & Frenking, G. (2006). *J. Org. Chem.*, *71*, 2251.
[31] Hansch, C., Leo, A., & Taft, R. W. (1991). *Chem. Rev.*, *97*, 165.
[32] Masui, H., & Lever, A. B. P. (1993). *Inorg. Chem.*, *32*, 2199.
[33] Pichot, F., Beck, J. H., & Elliott, C. M. (1999). *J. Phys. Chem. A*, *103*, 6263.
[34] Gillanders, F., Giordano, L., Díaz, S. A., Jovin, T. M., & Jares-Erijman, E. A. (2014), *Photochem. Photobiol. Sci.*, *13*, 603.
[35] Dogan, F., Mercimek, B., & Kaya I. (2010). *Chin. J. Chem.*, *28*, 1114.
[36] Maya, E. M., Benavente, J., & Abajo J. D. (2012). *Mater. Chem. Phys.*, *131*, 581.